A VEM-fully discrete polytopal scheme with bubble stabilisation for mixed-dimensional models with frictional contact at matrix–fracture interfaces

Roland Masson[1]
With: Ali Haidar[1], Jérôme Droniou[2], Guillaume Enchery[3], Isabelle Faille[3]

(1) LJAD, Université Côte d'Azur, Inria, CNRS
(2) IMAG, Université de Montpellier, CNRS
(3) IFPEN

Workshop on the mathematical and numerical modeling of CO_2 storage
january 31- february 02 2024

Fractured/faulted poro-mechanical models: applications

- CO2 sequestration
  - Fault/fracture reactivation
    - Leakage
    - Induced seismicity
- Other applications
  - Geothermal systems
  - Radioactive waste geological repositories
  - H_2 storage

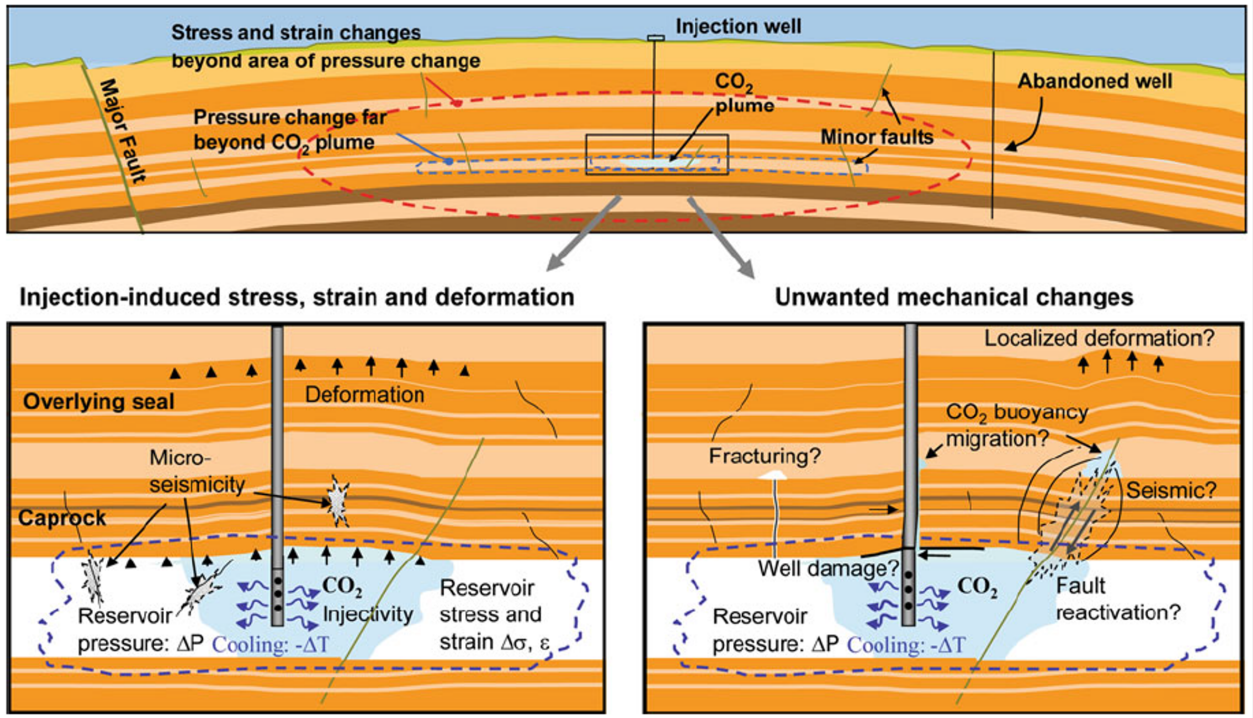

Tiré de *"The Geomechanics of CO2 Storage in Deep Sedimentary Formations, Jonny Rutqvist Geotech Geol Eng (2012) 30:525–551 DOI 10.1007/s10706-011-9491-0 »*

Typical meshes in geosciences

Corner Point Geometries (CPG)

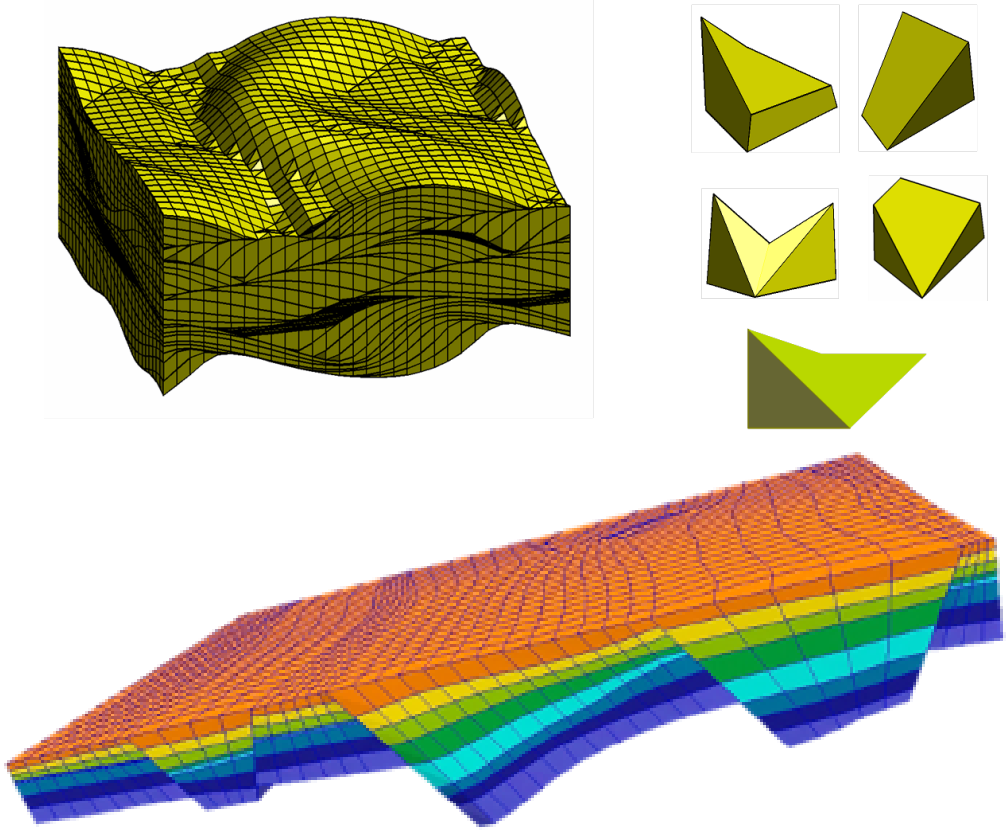

- Not adapted to Finite Element Methods (FEM) typically used in Mechanics
- Need for discretizations of contact mechanics adapted to **polyhedral** meshes

Outline

1. Contact-Mechanical model

2. Discretization on polyhedral meshes

3. Numerical validation
   - Contact-mechanics
   - Poromechanics

Static contact mechanical problem

- The matrix and fracture pressures p_m and p_f are fixed
- Isotropic linear poroelastic model in the matrix domain $\Omega \setminus \Gamma$

$$\begin{cases} -\mathrm{div}\Big(\sigma^T(\mathbf{u}, p_m)\Big) = \mathbf{f}, \\ \sigma^T(\mathbf{u}, p_m) = \sigma(\mathbf{u}) - b\ p_m\ \mathbb{I}, \\ \sigma(\mathbf{u}) = 2\mu\ \mathfrak{e}(\mathbf{u}) + \lambda\ \mathrm{div}\,\mathbf{u}\ \mathbb{I}. \end{cases}$$

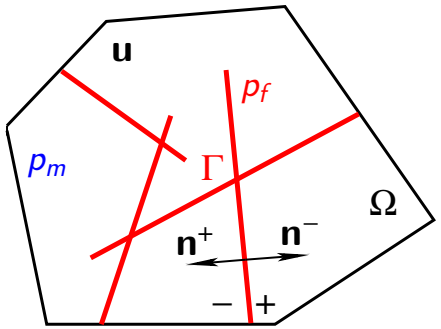

Mixed-dimensional geometry and unknowns

Fracture mechanical model on the fracture network Γ

Jumps : $[\![\mathbf{u}]\!] = \mathbf{u}^+ - \mathbf{u}^-,\ [\![\mathbf{u}]\!]_n = [\![\mathbf{u}]\!] \cdot \mathbf{n}^+,\ [\![\mathbf{u}]\!]_\tau = [\![\mathbf{u}]\!] - [\![\mathbf{u}]\!]_n \mathbf{n}^+,$

Surface Tractions: $\mathbf{T}^\pm = \sigma^T(\mathbf{u}, p_m)^\pm \mathbf{n}^\pm + p_f \mathbf{n}^\pm$

Law of Action and Reaction:

$$\mathbf{T}^+ + \mathbf{T}^- = \mathbf{0}$$

Non penetration conditions:

$$T_n^+ \leq 0, \quad [\![\mathbf{u}]\!]_n \leq 0, \quad [\![\mathbf{u}]\!]_n \ T_n^+ = 0$$

Coulomb friction conditions:

$$|\mathbf{T}_\tau^+| \leq -F \ T_n^+,$$

$$\mathbf{T}_\tau^+(\mathbf{u}) \cdot [\![\mathbf{u}]\!]_\tau - F \ T_n^+(\mathbf{u}) \, |[\![\mathbf{u}]\!]_\tau| = 0$$

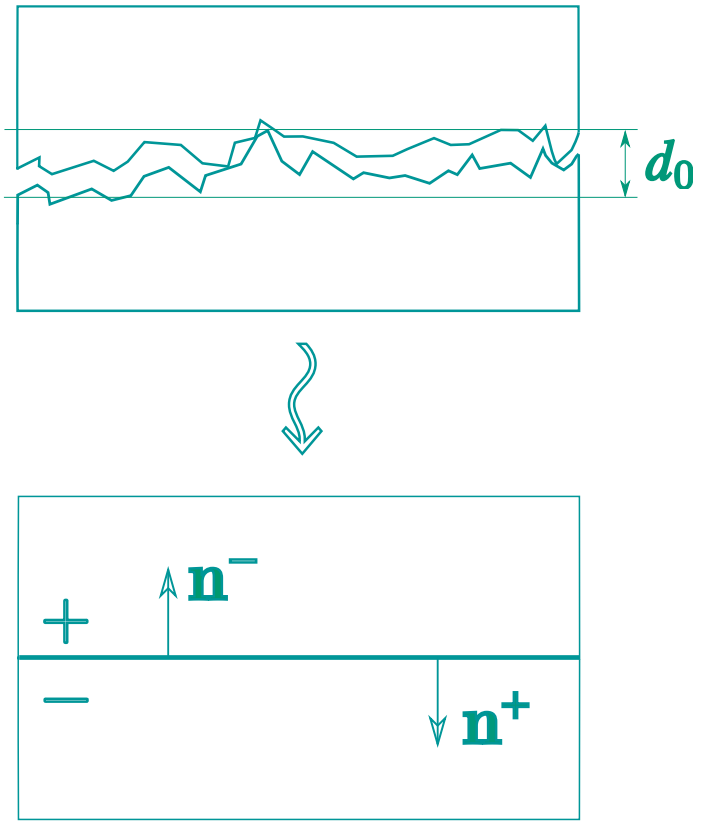

Mixed variational inequality

Lagrange multiplier: $\boldsymbol{\lambda} = -\mathbf{T}^+$

Dual cone of admissible Lagrange multipliers: given $\boldsymbol{\lambda} = (\lambda_{\mathbf{n}}, \boldsymbol{\lambda}_{\boldsymbol{\tau}})$

$$C_f(\lambda_{\mathbf{n}}) = \Big\{ \boldsymbol{\mu} \in (H^{-1/2}(\Gamma))^d \ : \ \mu_{\mathbf{n}} \geq 0, \ |\boldsymbol{\mu}_{\boldsymbol{\tau}}| \leq F\lambda_{\mathbf{n}} \quad \text{(in a weak sense)} \Big\}.$$

Mixed variational inequality: $\mathbf{u} \in H^1_0(\Omega \backslash \overline{\Gamma})^d$, $\boldsymbol{\lambda} \in C_f(\lambda_{\mathbf{n}})$ such that

$$\int_\Omega \Big(\varpi(\mathbf{u}) : \mathfrak{e}(\mathbf{v}) - b \ p_m \mathrm{div}(\mathbf{v}) \Big) + \langle \boldsymbol{\lambda}, [\![\mathbf{v}]\!] \rangle_\Gamma + \int_\Gamma p_f \ [\![\mathbf{v}]\!]_{\mathbf{n}} = \int_\Omega \mathbf{f} \cdot \mathbf{v},$$

$$\langle \boldsymbol{\mu} - \boldsymbol{\lambda}, [\![\mathbf{u}]\!] \rangle_\Gamma \leq 0,$$

for all $\mathbf{v} \in H^1_0(\Omega \backslash \overline{\Gamma})^d$, $\boldsymbol{\mu} \in C_f(\lambda_{\mathbf{n}})$.

Polyhedral nodal discretization of the displacement field **u**

- Virtual Element Method (VEM) [Beirao Da Veiga et al 2013]
- **Fully discrete approach** (nodal MFD, CDO, DDR)
  - local reconstruction operators from the space of discrete unknowns onto polynomial spaces.

Nodal displacement unknowns:

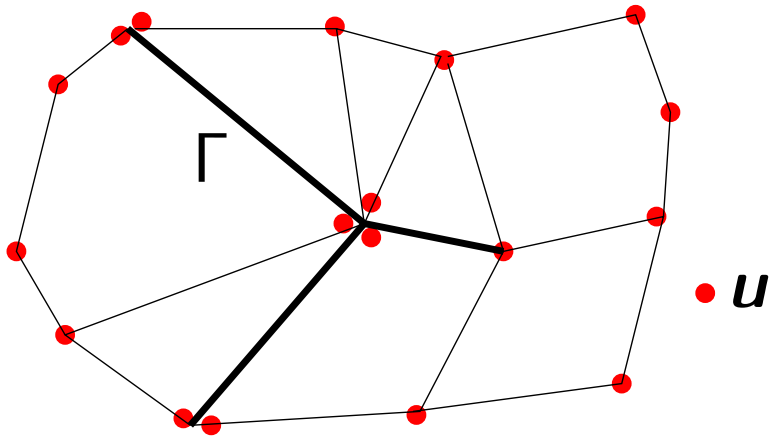

Extension to contact-mechanics: mixed formulation

- Mixed formulation with nodal Lagrange multipliers [Wriggers et al 2016]
- Mixed formulation with face-wise constant Lagrange multipliers $\boldsymbol{\lambda} = -\mathbf{T}^+$
  - deal with fracture networks including intersections
  - face-wise contact conditions
  - preserve the contact dissipative properties

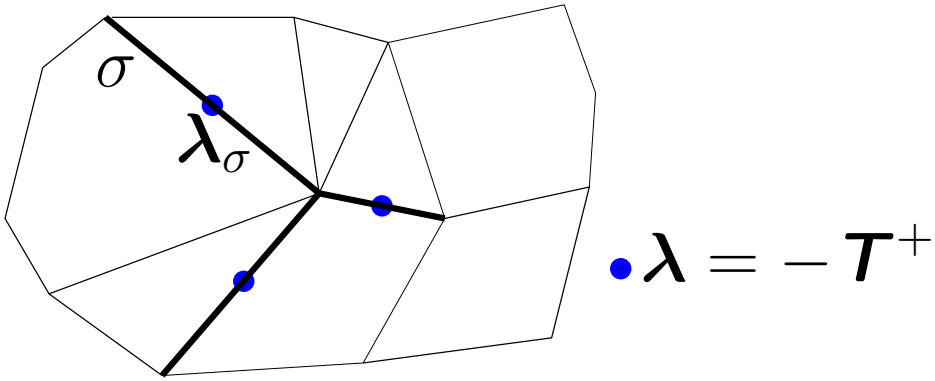

$$\mathbf{M}_{\mathcal{D}} = \left\{ \boldsymbol{\lambda}_{\mathcal{D}} \in L^2(\Gamma)^d \ : \ \boldsymbol{\lambda}_{\mathcal{D}}(\mathbf{x}) = \boldsymbol{\lambda}_\sigma \ \forall \sigma \in \mathcal{F}_\Gamma, \forall \ \mathbf{x} \in \sigma \right\}.$$

For $\boldsymbol{\lambda}_{\mathcal{D}} \in \mathbf{M}_{\mathcal{D}}$, we define the discrete dual cone of admissible Lagrange multipliers:

$$\mathbf{C}_{\mathcal{D}}\left(\lambda_{\mathcal{D},\mathbf{n}}\right) = \left\{ \boldsymbol{\mu}_{\mathcal{D}} = \left(\mu_{\mathcal{D},\mathbf{n}}, \boldsymbol{\mu}_{\mathcal{D},\boldsymbol{\tau}}\right) \in \mathbf{M}_{\mathcal{D}} \ : \ \mu_{\mathcal{D},\mathbf{n}} \geq 0, \ |\boldsymbol{\mu}_{\mathcal{D},\boldsymbol{\tau}}| \leq F\lambda_{\mathcal{D},\mathbf{n}} \right\}.$$

Stabilization of the Lagrange multiplier

A stabilization is required to avoid spurious Lagrange multiplier modes

- Enrichment of the displacement space
  - $\mathbb{P}^1$-bubble FEM [Renard et al 2003]
  - **In this work: polytopal bubble stabilisation**

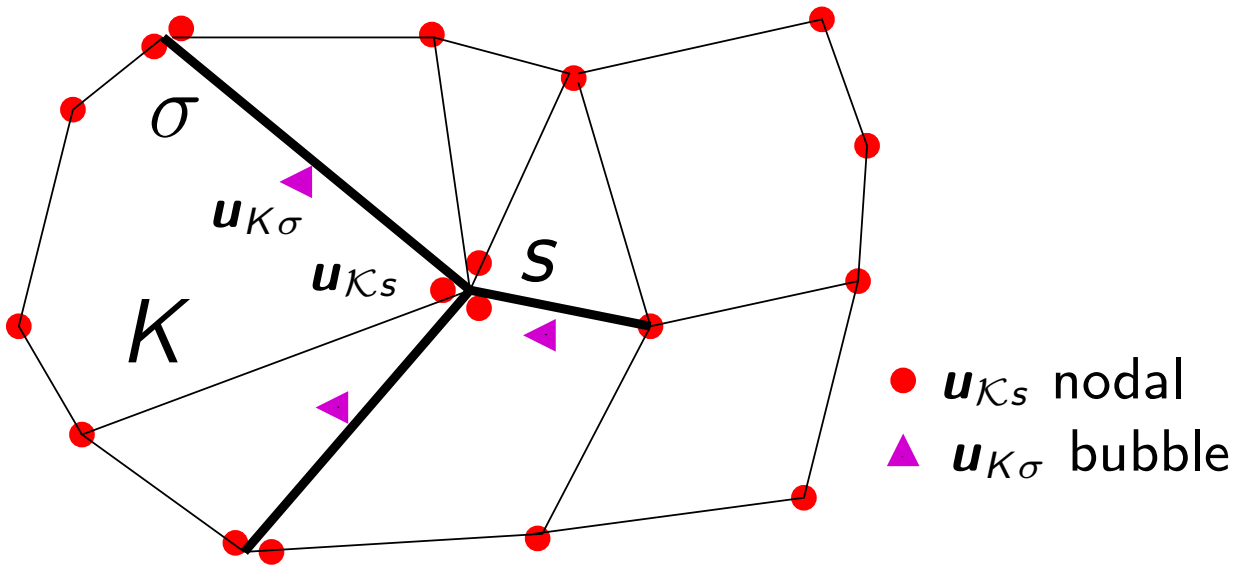

Vector space of discrete displacement unknowns:

$$\mathbf{U}_{\mathcal{D}} = \left\{ \mathbf{v}_{\mathcal{D}} = \left((\mathbf{v}_{\mathcal{K}s})_{\mathcal{K}s \in \overline{\mathcal{M}}_s, s \in \mathcal{V}}, (\mathbf{v}_{K\sigma})_{\sigma \in \mathcal{F}^+_{\Gamma,K},\ K \in \mathcal{M}} \right) \ : \ \mathbf{v}_{\mathcal{K}s} \in \mathbb{R}^d \ , \ \mathbf{v}_{K\sigma} \in \mathbb{R}^d \right\}$$

Interpolation operator

$$\mathcal{I}_{\mathcal{D}} : C^0(\Omega \setminus \overline{\Gamma})^d \to \mathbf{U}_{\mathcal{D}}$$

$$\begin{cases} (\mathcal{I}_{\mathcal{D}}\mathbf{u})_{\mathcal{K}s} = \mathbf{u}_{|K}(\mathbf{x}_s), \\ (\mathcal{I}_{\mathcal{D}}\mathbf{u})_{K\sigma} = \dfrac{1}{|\sigma|}\displaystyle\int_\sigma (\gamma^{K\sigma}\mathbf{u} - \Pi^{K\sigma}(\mathcal{I}_{\mathcal{D}}\mathbf{u})). \end{cases}$$

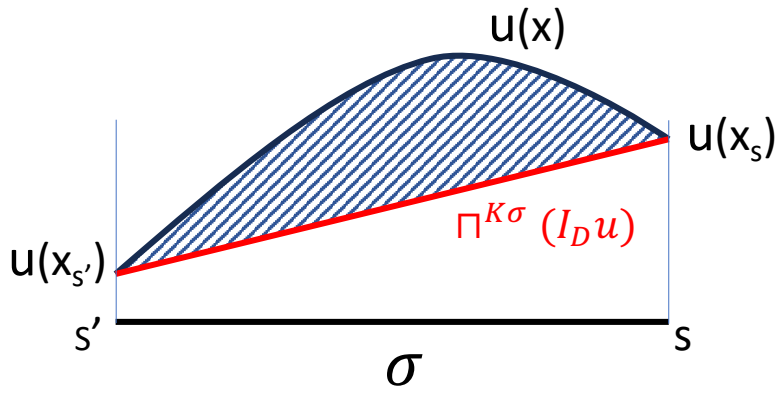

- $\gamma^{K\sigma}$ is the trace operator on σ from the K side
- $\Pi^{K\sigma}$ is the face linear reconstruction operator depending only on the nodal degrees of freedom

Reconstruction operators

Cell gradient and function reconstruction operators:

- $\nabla^K : \mathbf{U}_{\mathcal{D}} \to (\mathbb{P}^0(K))^{d\times d}$
- $\Pi^K : \mathbf{U}_{\mathcal{D}} \to (\mathbb{P}^1(K))^d$

Fracture face mean displacement jump:

- $[\![\ ]\!]_\sigma : \mathbf{U}_{\mathcal{D}} \to \mathbb{P}^0(\sigma)^d$

Global piecewise reconstruction operators:

- $(\mathfrak{e}_{\mathcal{D}}(\mathbf{u}_{\mathcal{D}}))|_K = \frac{1}{2}(\nabla^K \mathbf{u}_{\mathcal{D}} + {}^t\nabla^K \mathbf{u}_{\mathcal{D}})$
- $\mathrm{div}_{\mathcal{D}} = \mathrm{tr}(\mathfrak{e}_{\mathcal{D}}), \quad \mathfrak{s}_{\mathcal{D}} = 2\mu\ \mathfrak{e}_{\mathcal{D}} + \lambda\ \mathrm{div}_{\mathcal{D}}\ \mathbb{I}$
- $(\Pi_{\mathcal{D}}\mathbf{u}_{\mathcal{D}})|_K = \Pi^K \mathbf{u}_{\mathcal{D}}$
- $([\![\mathbf{u}_{\mathcal{D}}]\!]_{\mathcal{D}})|_\sigma = [\![\mathbf{u}_{\mathcal{D}}]\!]_\sigma$

Discrete mixed variational formulation

Find $(\mathbf{u}_\mathcal{D}, \boldsymbol{\lambda}_\mathcal{D}) \in \mathbf{U}^0_\mathcal{D} \times \mathbf{C}_\mathcal{D}(\lambda_{\mathcal{D},\mathbf{n}})$, such that:

$$\begin{cases} \displaystyle\int_\Omega \mathfrak{o}_\mathcal{D}(\mathbf{u}_\mathcal{D}) : \mathfrak{e}_\mathcal{D}(\mathbf{v}_\mathcal{D}) + S_{\mu,\lambda,\mathcal{D}}(\mathbf{u}_\mathcal{D}, \mathbf{v}_\mathcal{D}) - \int_\Omega b\, p_m \,\mathrm{div}_\mathcal{D}\mathbf{v}_\mathcal{D} \\ \displaystyle + \int_\Gamma p_f [\![\mathbf{v}_\mathcal{D}]\!]_{\mathcal{D},\mathbf{n}} + \int_\Gamma \boldsymbol{\lambda}_\mathcal{D} \cdot [\![\mathbf{v}_\mathcal{D}]\!]_\mathcal{D} = \sum_{K\in\mathcal{M}} \frac{1}{|K|} \int_K \mathbf{f} \cdot \int_K \Pi_\mathcal{D}\mathbf{v}_\mathcal{D}, \\ \\ \displaystyle\int_\Gamma (\boldsymbol{\mu}_\mathcal{D} - \boldsymbol{\lambda}_\mathcal{D}) \cdot [\![\mathbf{u}_\mathcal{D}]\!]_\mathcal{D} \le 0, \end{cases}$$

for all $(\mathbf{v}_\mathcal{D}, \boldsymbol{\mu}_\mathcal{D}) \in \mathbf{U}^0_\mathcal{D} \times \mathbf{C}_\mathcal{D}(\lambda_{\mathcal{D},\mathbf{n}})$.

The variational inequality can be reformulated by local to each fracture face equations:

$$\begin{cases} \lambda_{\sigma,\mathbf{n}} = \left[\lambda_{\sigma,\mathbf{n}} + \beta_{\sigma,\mathbf{n}} [\![\mathbf{u}_\mathcal{D}]\!]_{\sigma,\mathbf{n}}\right]_{\mathbb{R}^+} \\ \boldsymbol{\lambda}_{\sigma,\boldsymbol{\tau}} = \left[\boldsymbol{\lambda}_{\sigma,\boldsymbol{\tau}} + \beta_{\sigma,\boldsymbol{\tau}} [\![\mathbf{u}_\mathcal{D}]\!]_{\sigma,\boldsymbol{\tau}}\right]_{F\lambda_{\sigma,\mathbf{n}}} \end{cases}$$

with $[x]_{\mathbb{R}^+} = \max\{0, x\}$ and $[\mathbf{x}]_\alpha = \begin{cases} \mathbf{x} & \text{if } |\mathbf{x}| \le \alpha, \\ \alpha \dfrac{\mathbf{x}}{|\mathbf{x}|} & \text{otherwise,} \end{cases}$ $\beta_{\mathcal{D},\mathbf{n}} > 0, \quad \beta_{\mathcal{D},\boldsymbol{\tau}} > 0.$

Jump reconstruction operator on a face σ: $[\![\ ]\!]_\sigma$

Face mean value reconstruction:

$$\overline{\mathbf{v}}_{K\sigma} = \sum_{s\in\mathcal{V}_\sigma} \omega_s^\sigma \mathbf{v}_{\mathcal{K}s}$$

with the face center of mass $\overline{\mathbf{x}}_\sigma = \sum_{s\in\mathcal{V}_\sigma} \omega_s^\sigma \mathbf{x}_s$.

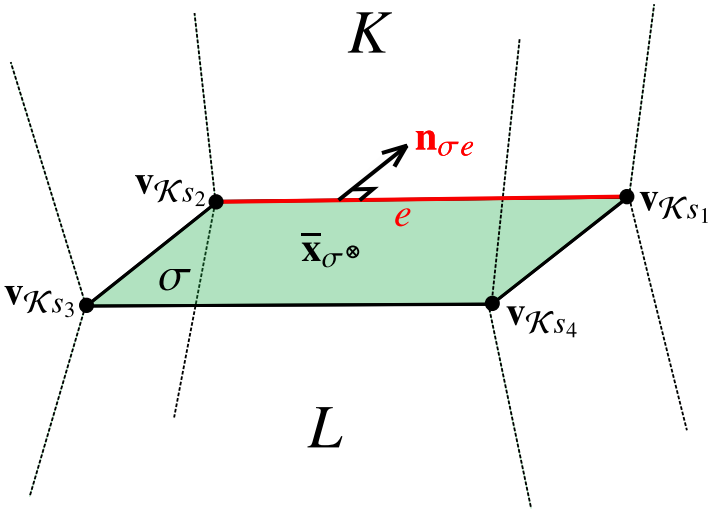

Face average displacement jump operator:

$$[\![\ ]\!]_\sigma : \mathbf{U}_\mathcal{D} \to \mathbb{P}^0(\sigma)^d$$

$$[\![\mathbf{v}_\mathcal{D}]\!]_\sigma = \overline{\mathbf{v}}_{K\sigma} - \overline{\mathbf{v}}_{L\sigma} + \mathbf{v}_{K\sigma}.$$

Discrete reconstruction operators in K: ∇^K

The gradient reconstruction operator:

$$\nabla^K : \mathbf{U}_{\mathcal{D}} \to (\mathbb{P}^0(K))^{d\times d}$$

$$\nabla^K \mathbf{v}_{\mathcal{D}} = \frac{1}{|K|} \sum_{\sigma\in\mathcal{F}^+_{\Gamma,K}} |\sigma| \mathbf{v}_{K\sigma} \otimes \mathbf{n}_{K\sigma} + \frac{1}{|K|} \sum_{\sigma\in\mathcal{F}_K} |\sigma| \overline{\mathbf{v}}_{K\sigma} \otimes \mathbf{n}_{K\sigma}.$$

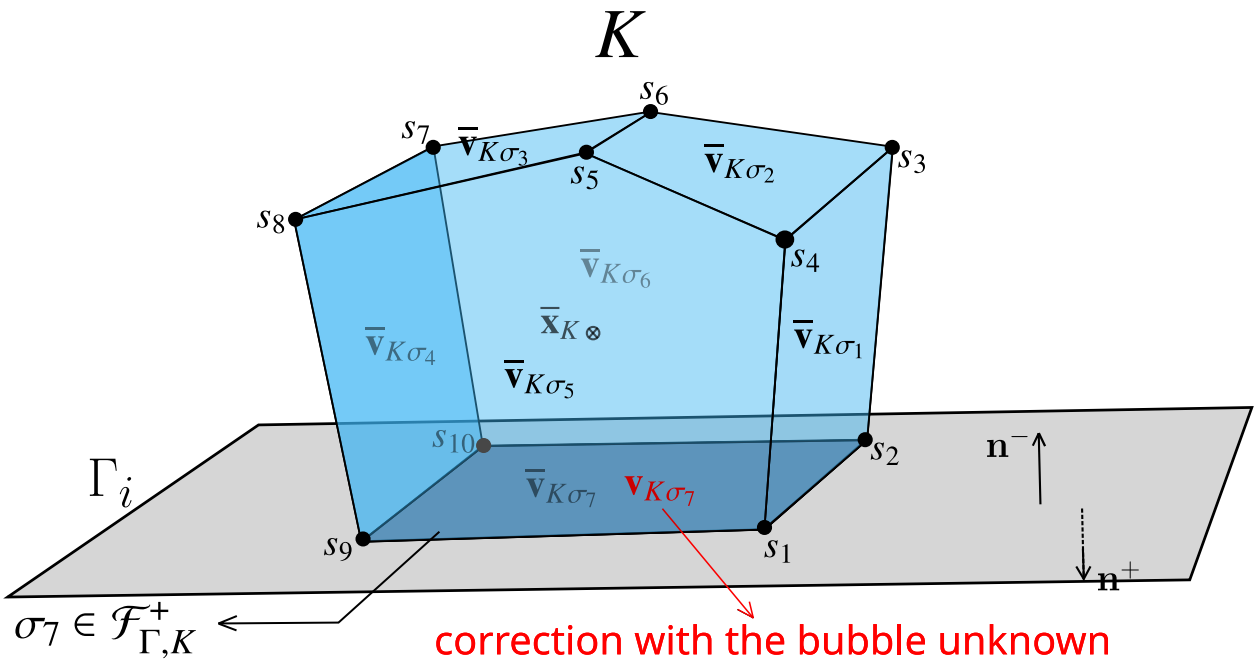

Figure: Nodal and bubble unknowns in a cell K

Discrete reconstruction operators in K: Π^K

Linear function reconstruction operator:

$$\Pi^K : \mathbf{U}_{\mathcal{D}} \to (\mathbb{P}^1(K))^d$$

$$\Pi^K \mathbf{v}_{\mathcal{D}}(\mathbf{x}) = \nabla^K \mathbf{v}_{\mathcal{D}} \, (\mathbf{x} - \overline{\mathbf{x}}_K) + \overline{\mathbf{v}}_K,$$

with

$$\overline{\mathbf{v}}_K = \sum_{s \in \mathcal{V}_K} \omega_s^K \mathbf{v}_{\mathcal{K}s}$$

and the cell center of mass $\overline{\mathbf{x}}_K = \sum_{s \in \mathcal{V}_K} \omega_s^K \mathbf{x}_s$.

Stabilisation term (*dofi-dofi* approach)

$S_{\mu,\lambda,\mathcal{D}}$ is the scaled stabilisation bilinear form defined by:

$$S_{\mu,\lambda,\mathcal{D}}(\mathbf{u}_{\mathcal{D}},\mathbf{v}_{\mathcal{D}}) = \sum_{K\in\mathcal{M}} h_K^{d-2}(2\mu_K+\lambda_K)S_K(\mathbf{u}_{\mathcal{D}},\mathbf{v}_D),$$

with

$$S_K(\mathbf{u}_{\mathcal{D}},\mathbf{v}_{\mathcal{D}}) = \sum_{s\in\mathcal{V}_K}(\mathbf{u}_{\mathcal{K}s}-\Pi^K\mathbf{u}_{\mathcal{D}}(\mathbf{x}_s))\cdot(\mathbf{v}_{\mathcal{K}s}-\Pi^K\mathbf{v}_{\mathcal{D}}(\mathbf{x}_s)) + \sum_{\sigma\in\mathcal{F}^+_{\Gamma,K}} \mathbf{u}_{K\sigma}\cdot\mathbf{v}_{K\sigma},$$

such that

$$S_K(\mathcal{I}_{\mathcal{D}}\mathbf{q},\mathbf{v}_{\mathcal{D}}) = S_K(\mathbf{u}_{\mathcal{D}},\mathcal{I}_{\mathcal{D}}\mathbf{q}) = 0$$

for all $\mathbf{q}\in\mathbb{P}^1(K)$.

Error estimate for Tresca friction

Let $(\mathbf{u}, \boldsymbol{\lambda})$ be the exact solution and assume that $\mathbf{u} \in H^2(\mathcal{M})$ and $\boldsymbol{\lambda} \in H^1(\mathcal{F}_\Gamma)$. Then the discrete solution $(\mathbf{u}_\mathcal{D}, \boldsymbol{\lambda}_\mathcal{D})$ satisfies the following error estimate:

$$\|\nabla^\mathcal{D} \mathbf{u}_\mathcal{D} - \nabla \mathbf{u}\|_{L^2(\Omega\setminus\overline{\Gamma})} + \|\boldsymbol{\lambda}_\mathcal{D} - \boldsymbol{\lambda}\|_{-1/2,\Gamma} \lesssim h_\mathcal{D}(|\boldsymbol{\lambda}|_{H^1(\mathcal{F}_\Gamma)} + |\mathbf{u}|_{H^2(\mathcal{M})}).$$

The proof is mainly based on the **discrete inf-sup condition**:

$$\sup_{\mathbf{v}_\mathcal{D} \in \mathbf{U}^0_\mathcal{D}} \frac{\int_\Gamma \boldsymbol{\lambda}_\mathcal{D} \cdot [\![\mathbf{v}_\mathcal{D}]\!]_\mathcal{D}}{\|\mathbf{v}_\mathcal{D}\|_{1,\mathcal{D}}} \gtrsim \|\boldsymbol{\lambda}_\mathcal{D}\|_{-1/2,\Gamma} \qquad \forall \boldsymbol{\lambda}_\mathcal{D} \in \mathbf{M}_\mathcal{D}.$$

with $\|\mathbf{v}_\mathcal{D}\|_{1,\mathcal{D}} := \left(\sum_{K \in \mathcal{M}} (\|\nabla^K \mathbf{v}_\mathcal{D}\|^2_{L^2(K)} + S_K(\mathbf{v}_\mathcal{D}, \mathbf{v}_\mathcal{D})) \right)^{1/2}$.

and the **discrete Korn inequality**:

$$\|\mathbf{v}_\mathcal{D}\|^2_{1,\mathcal{D}} \lesssim \|\mathfrak{E}_\mathcal{D}(\mathbf{v}_\mathcal{D})\|^2_{L^2(\Omega\setminus\overline{\Gamma})} + \sum_{K \in \mathcal{M}} S_K(\mathbf{v}_\mathcal{D}, \mathbf{v}_\mathcal{D}) \qquad \forall \mathbf{v}_\mathcal{D} \in \mathbf{U}^0_\mathcal{D}.$$

Manufactured solution for a frictionless contact mechanical model

Frictionless contact mechanical model:

$$\begin{cases} -\mathrm{div}\sigma(\mathbf{u}) = \mathbf{f} & \text{on } \Omega\backslash\overline{\Gamma} \\ \sigma(\mathbf{u}) = 2\mu\ \epsilon(\mathbf{u}) + \lambda\ \mathrm{div}\,\mathbf{u}\ \mathbb{I} & \text{on } \Omega\backslash\overline{\Gamma} \\ \mathbf{T}^+ + \mathbf{T}^- = \mathbf{0} & \text{on } \Gamma \\ T_n \le 0,\ [\![\mathbf{u}]\!]_n \le 0,\ [\![\mathbf{u}]\!]_n\ T_n = 0 & \text{on } \Gamma \\ \mathbf{T}_\tau = \mathbf{0} & \text{on } \Gamma. \end{cases}$$

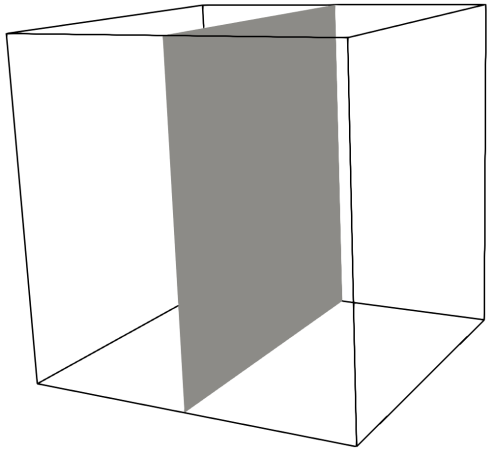

Analytical solution:

$$\mathbf{u}(x,y,z) = \begin{cases} \begin{pmatrix} g(x,y)p(z) \\ p(z) \\ x^2 p(z) \end{pmatrix} & \text{if } z \ge 0, \\ \begin{pmatrix} h(x)p^+(z) \\ h(x)\left(p^+(z)\right)' \\ -\int_0^x h(\xi)\mathrm{d}\xi\,\left(p^+(z)\right)' \end{pmatrix} & \text{if } z < 0,\ x\ < 0, \\ \begin{pmatrix} h(x)p^-(z) \\ h(x)\left(p^-(z)\right)' \\ -\int_0^x h(\xi)\mathrm{d}\xi\,\left(p^-(z)\right)' \end{pmatrix} & \text{if } z < 0,\ x\ \ge 0, \end{cases} \quad \text{with} \quad \begin{cases} g(x,y) = -\sin(\frac{\pi x}{2})\cos(\frac{\pi y}{2}) \\ p(z) = z^2 \\ h(x) = \cos(\frac{\pi x}{2}) \\ p^+(z) = z^4 \\ p^-(z) = 2z^4 \end{cases}$$

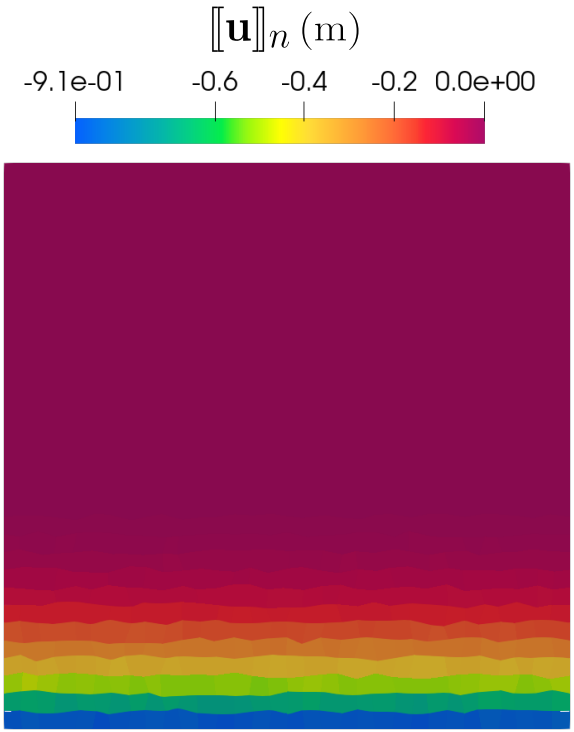
$[\![\mathbf{u}]\!]_n$ (m)
-9.1e-01
-0.6
-0.4
-0.2
0.0e+00
Z
X
Y

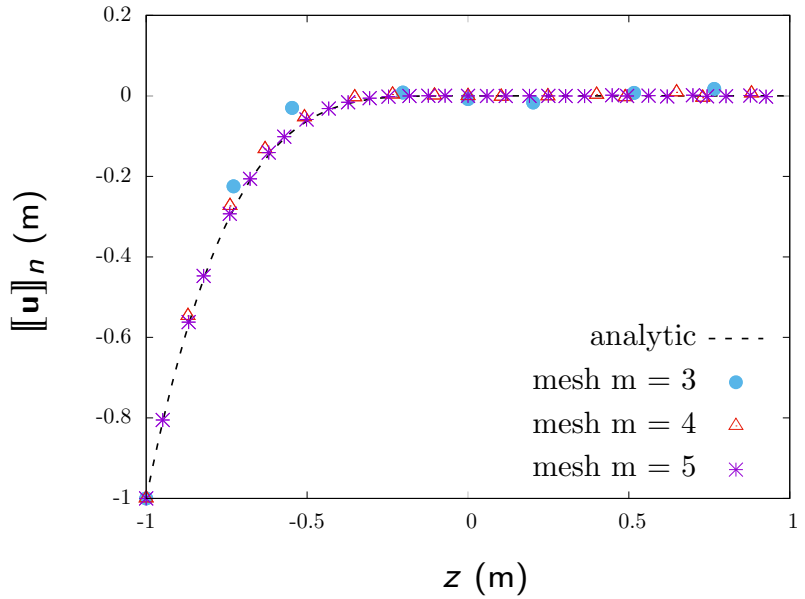
$[\![\mathbf{u}]\!]_n$ (m)
0.2
0
-0.2
-0.4
-0.6
-0.8
-1
-1
-0.5
0
0.5
1
z (m)
analytic
mesh m = 3
mesh m = 4
mesh m = 5

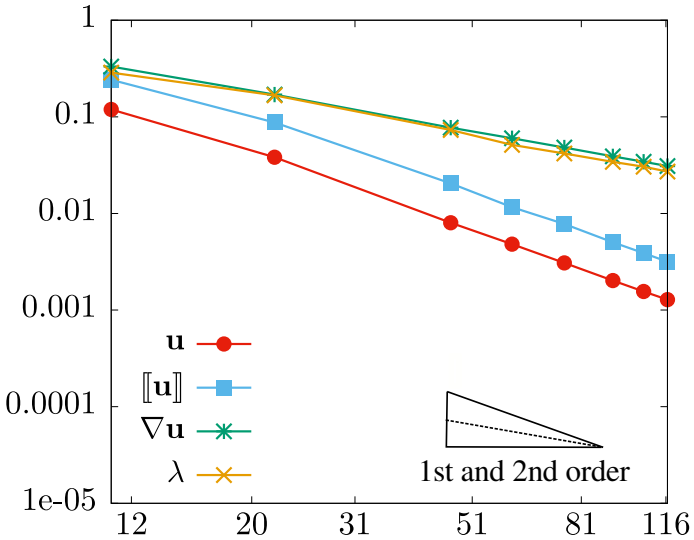

(a)

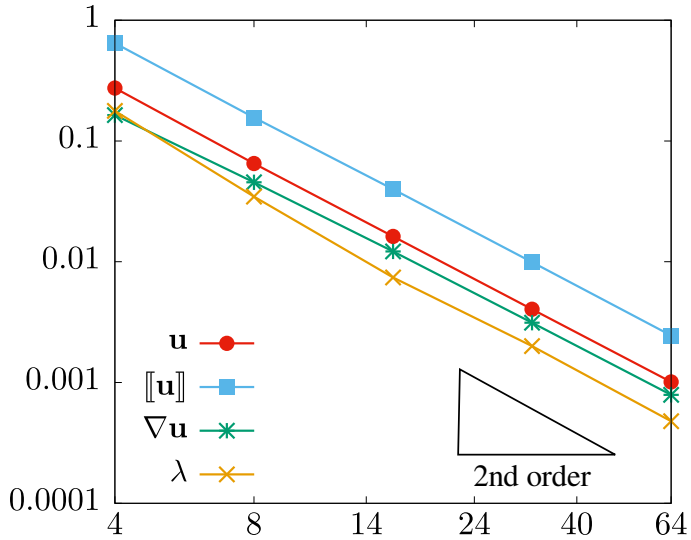

(b)

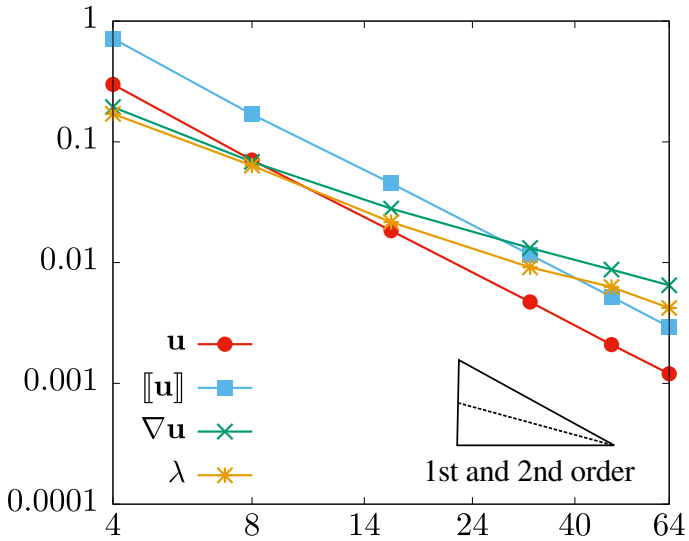

(c)

Figure: Error and convergence rates obtained with the VEM $\mathbb{P}^1$-bubble method: Tetrahedral mesh (a), cartesian mesh (b), polytopal mesh (c).

Single crack under compression

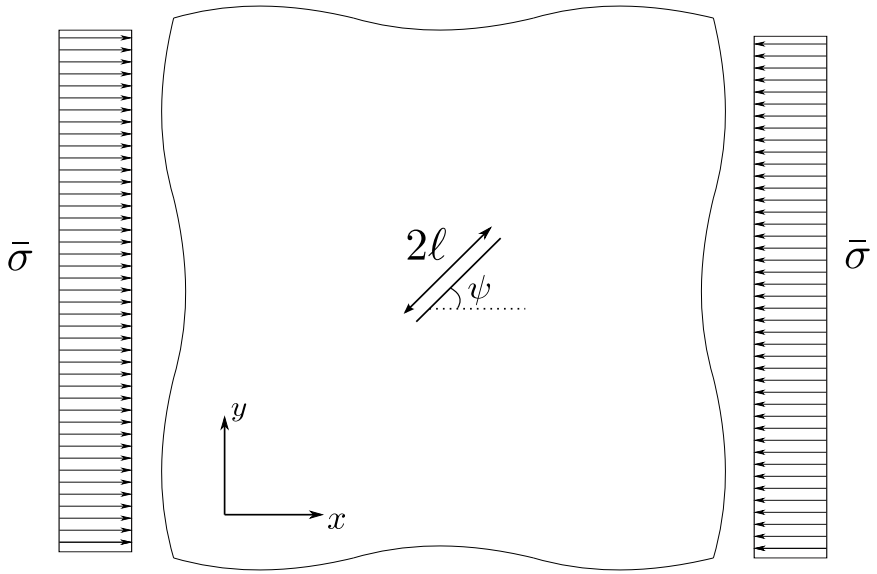

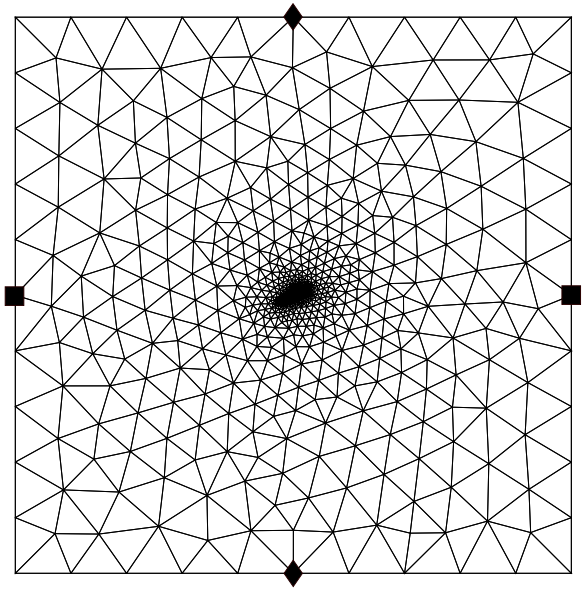

♦: $u_x = 0$, ■: $u_y = 0$

$$|\,[\![\bar{\mathbf{u}}]\!]_\tau(\tau)\,| = \frac{4(1-\nu)}{E}(\bar{\sigma}\sin\psi(\cos\psi - F\sin\psi))\sqrt{\ell^2 - (\ell^2-\tau^2)},$$

$$\bar{\lambda}_n(\tau) = \bar{\sigma}\sin^2\psi, \qquad 0 \le \tau \le 2\ell$$

Single crack under compression

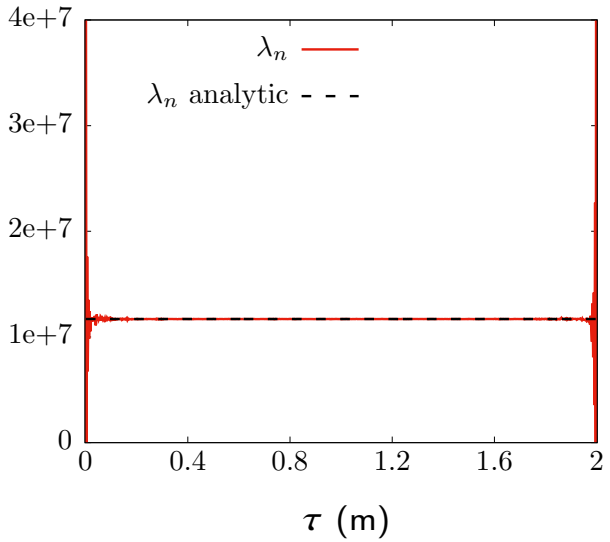

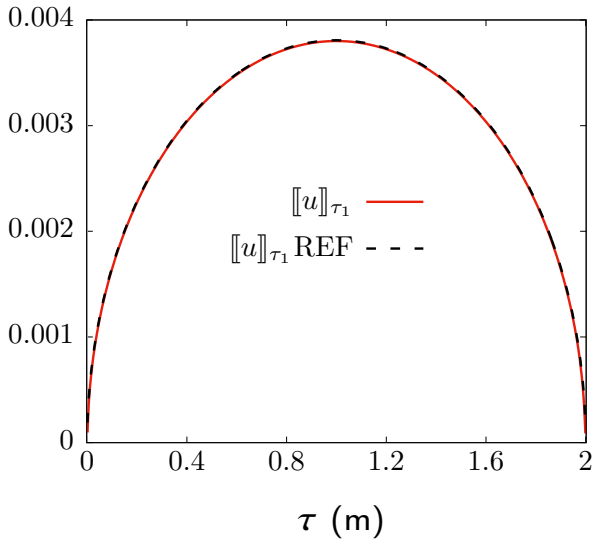

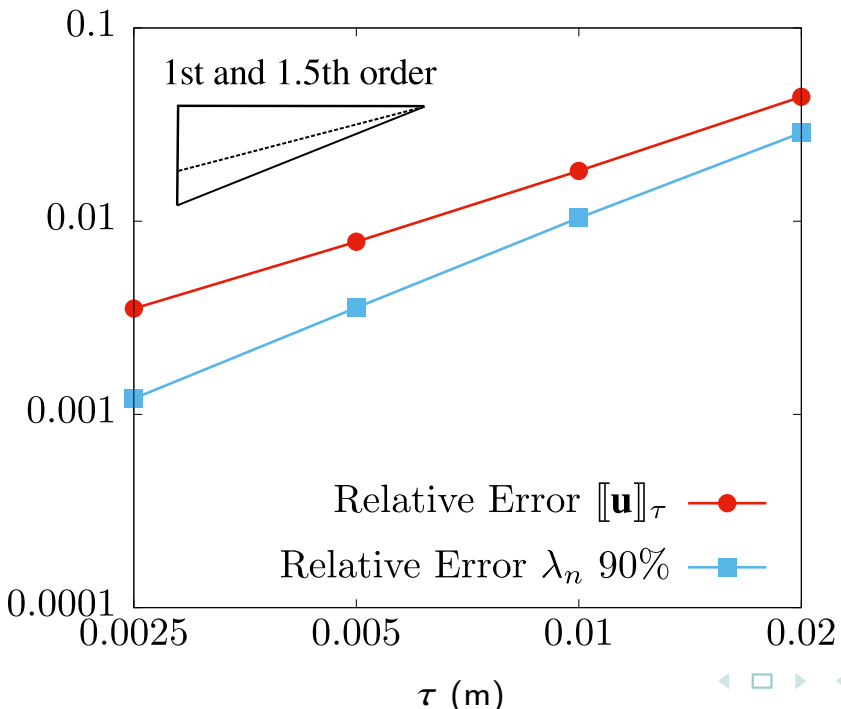

Coupling with a mixed-dimensional single phase Darcy flow

$$
\begin{cases}
\partial_t \phi_m + \operatorname{div} \mathbf{V}_m = h_m & \text{on } (0,T)\times\Omega\backslash\overline{\Gamma}, \\
\mathbf{V}_m = -\frac{\mathbb{K}_m}{\eta}\nabla p_m & \text{on } (0,T)\times\Omega\backslash\overline{\Gamma}, \\
\partial_t \mathrm{d}_f + \operatorname{div}_\tau \mathbf{V}_f - [\![\mathbf{V}_m]\!]_n = h_f & \text{on } (0,T)\times\Gamma, \\
\mathbf{V}_f = \frac{C_f(\mathrm{d}_f)}{\eta}\nabla_\tau p_f, & \text{on } (0,T)\times\Gamma, \\
\mathbf{V}_m^{\pm}\cdot\mathbf{n}^{\pm} = T_f(\mathrm{d}_f)(\gamma^{\pm} p_m - p_f) & \text{on } (0,T)\times\Gamma,
\end{cases}
$$

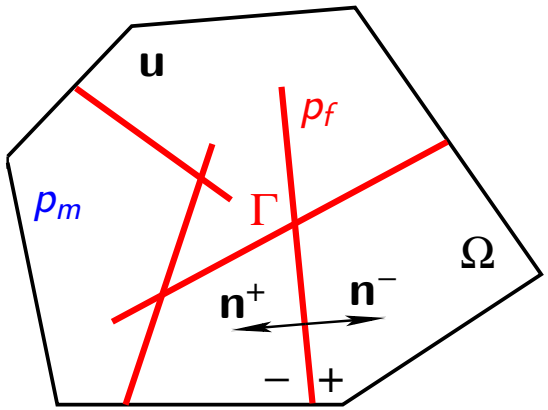

with the following coupling laws

$$
\begin{cases}
\partial_t \phi_m = b \operatorname{div}(\partial_t \mathbf{u}) + \frac{1}{M}\partial_t p_m & \text{on } (0,T)\times\Omega\backslash\overline{\Gamma}, \\
\mathrm{d}_f = \mathrm{d}_f^c - [\![\mathbf{u}]\!]_{\mathbf{n}} & \text{on } (0,T)\times\Gamma,
\end{cases}
$$

Hybrid Finite Volume (HFV) disctretization for the Darcy flow model [Brenner et al 2016]

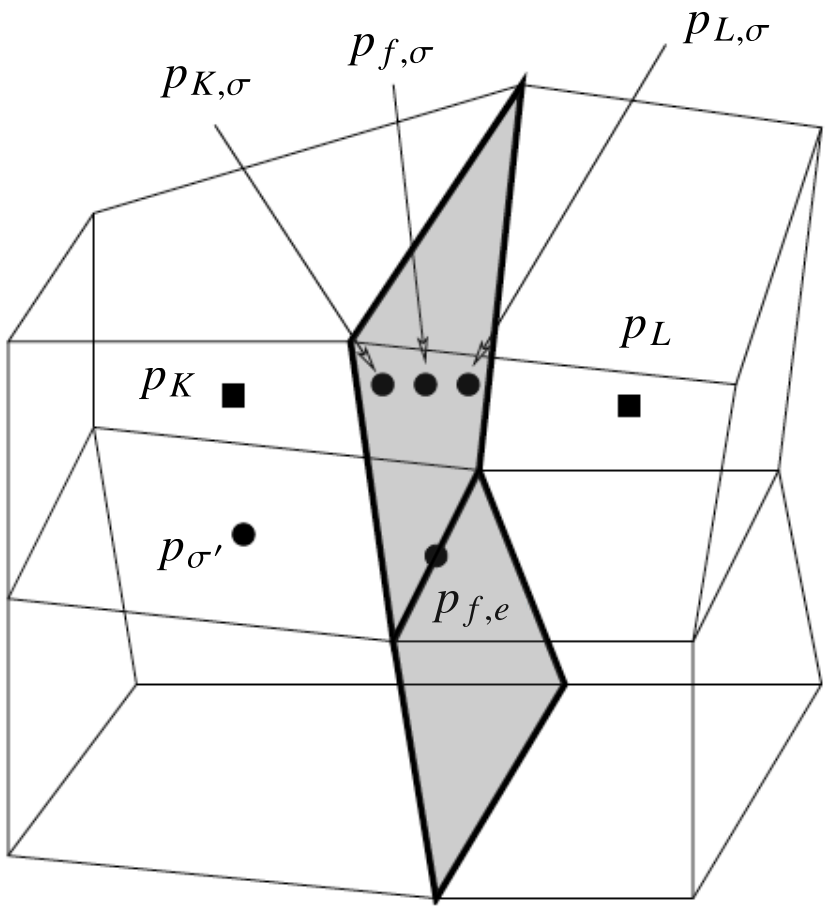

Figure: Pressure unknowns for the HFV scheme with discontinuous pressure

Discrete energy estimate

Any solution $\left(p^n_{\mathcal{D}}, \mathbf{u}^n_{\mathcal{D}}, \lambda^n_D)\right) \in X^0_{\mathcal{D}} \times \mathbf{U}^0_{\mathcal{D}} \times \mathbf{C}_{\mathcal{D}}(\lambda^n_{\mathcal{D},\mathbf{n}})$ for $n = 1, \cdots, N$ of the fully coupled scheme satisfies the following discrete energy estimates:

$$\delta^n_t \int_\Omega \frac{1}{2}\left(\varpi_{\mathcal{D}}(\mathbf{u}_{\mathcal{D}}) : \mathfrak{e}_{\mathcal{D}}(\mathbf{u}_{\mathcal{D}}) + S_{\mu,\lambda,\mathcal{D}}(\mathbf{u}_{\mathcal{D}}, \mathbf{u}_{\mathcal{D}}) + \frac{1}{M}|\Pi_{\mathcal{D}_m} p_{\mathcal{D}_m}|^2\right) + \int_\Gamma F\lambda^n_{\mathcal{D},\mathbf{n}} |[\![\delta^n_t \mathbf{u}_{\mathcal{D}}]\!]_{\mathcal{D},\tau}|$$

$$+ \int_\Omega \frac{\mathbb{K}_m}{\eta} \nabla_{\mathcal{D}_m} p^n_{\mathcal{D}_m} \cdot \nabla_{\mathcal{D}_m} p^n_{\mathcal{D}_m} + \int_\Gamma \frac{C^{n-1}_{f,\mathcal{D}}}{\eta} |\nabla_{\mathcal{D}_f} p^n_{\mathcal{D}_f}|^2 + \sum_{\mathfrak{a}\in\{+,-\}} \int_\Gamma \Lambda^{n-1}_{f,\mathcal{D}} ([\![p^n_{\mathcal{D}}]\!]^{\mathfrak{a}}_{\mathcal{D}})^2$$

$$\leq \int_\Omega h_m \Pi_{\mathcal{D}_m} p^n_{\mathcal{D}_m} + \int_\Gamma h_f \nabla_{\mathcal{D}_f} p^n_{\mathcal{D}_f} + \sum_{K\in\mathcal{M}} \int_K \mathbf{f}^n_K \cdot \Pi_{\mathcal{D}} \delta^n_t \mathbf{u}_{\mathcal{D}}.$$

Thanks to the dissipative property of the contact term:

$$\int_\Gamma \lambda^n_{\mathcal{D}} \cdot [\![\delta^n_t \mathbf{u}_{\mathcal{D}}]\!]_{\mathcal{D}} \geq \int_\Gamma F\lambda^n_{\mathcal{D},\mathbf{n}} |[\![\delta^n_t \mathbf{u}_{\mathcal{D}}]\!]_{\mathcal{D},\tau}| \geq 0.$$

2D DFM poromechanical test case

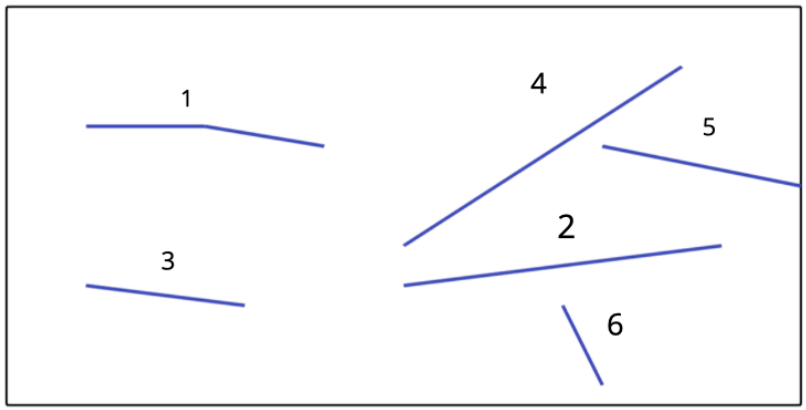

Anisotropic permeability tensor:

$$\mathbb{K}_m = 10^{-15}\left(\mathbf{e}_x \otimes \mathbf{e}_x + \frac{1}{2}\,\mathbf{e}_y \otimes \mathbf{e}_y\right)$$

Fracture aperture in contact state:

$$d_f^c(\mathbf{x}) = 10^{-4}\,\frac{\sqrt{\arctan(aD_i(\mathbf{x}))}}{\sqrt{\arctan(a\ell_i)}}, \quad i \in \{1,\ldots,6\}$$

$F = 0.5,\ b = 0.5,\ E = 10$ GPa, $\nu = 0.2$

No analytical solution available
$\Rightarrow$ Compute reference solution on fine mesh

[Acknowledgement: E. Keilegavlen (Bergen)]

Initial conditions

Initial pressures $p_m^0 = p_f^0 = 10^5$ Pa

Boundary conditions

Mechanics

Top boundary:

$$\mathrm{u}(t,\mathrm{x}) = \begin{cases} t\,[0.005\,\mathrm{m}, -0.002\,\mathrm{m}]\,4t/T & \text{if } t \le T/4 \\ t\,[0.005\,\mathrm{m}, -0.002\,\mathrm{m}] & \text{otherwise} \end{cases}$$

Bottom boundary: $\mathbf{u}(t,\mathbf{x}) \equiv \mathbf{0}$
Left and right boundaries: $\boldsymbol{\sigma}^T(t,\mathbf{x})\mathbf{n}(\mathbf{x}) \equiv \mathbf{0}$

Flow

Left boundary: $p_m(t,\mathbf{x}) \equiv p_m^0 = 10^5$ Pa

All other boundaries: impervious

Matrix over pressures

End of Stage 1 at $t = \frac{T}{4}$

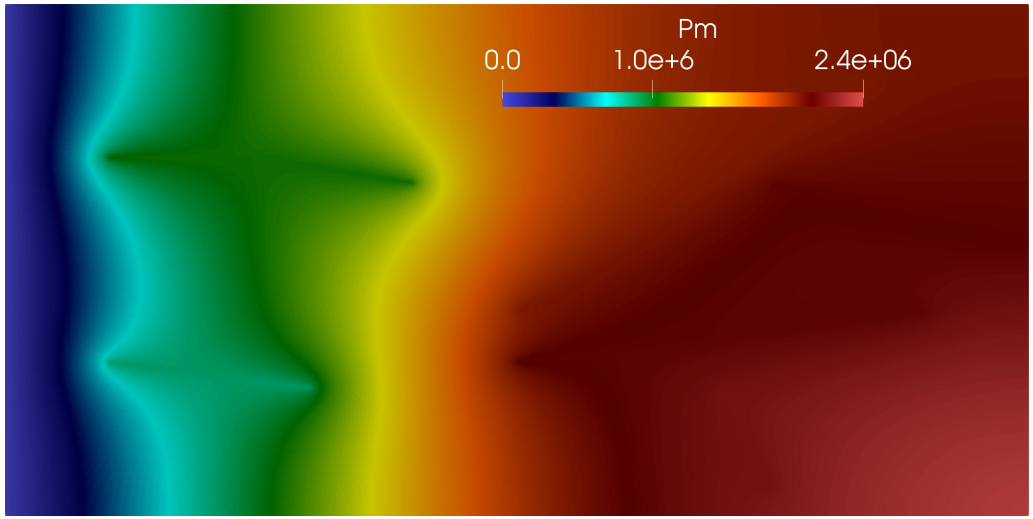

End of Stage 2 at $t = T$

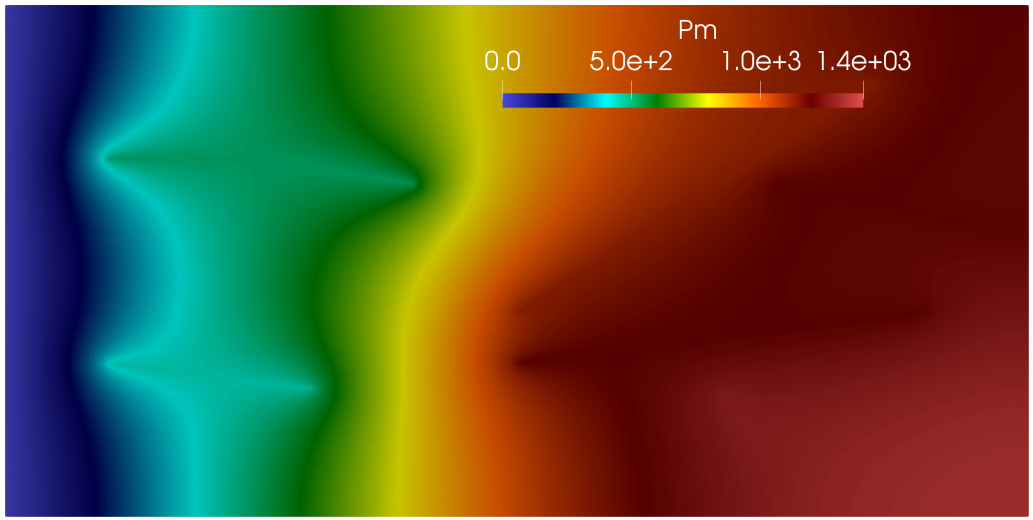

Contact state along the fractures

- $-\mathbf{T}_n = -(\sigma(\mathbf{u}) \cdot \mathbf{n}) \cdot \mathbf{n} - (1-b)p_f \quad and \quad |\mathbf{T}_\tau| \leq -F\ T_n$

End of Stage 1 at $t = \frac{T}{4}$

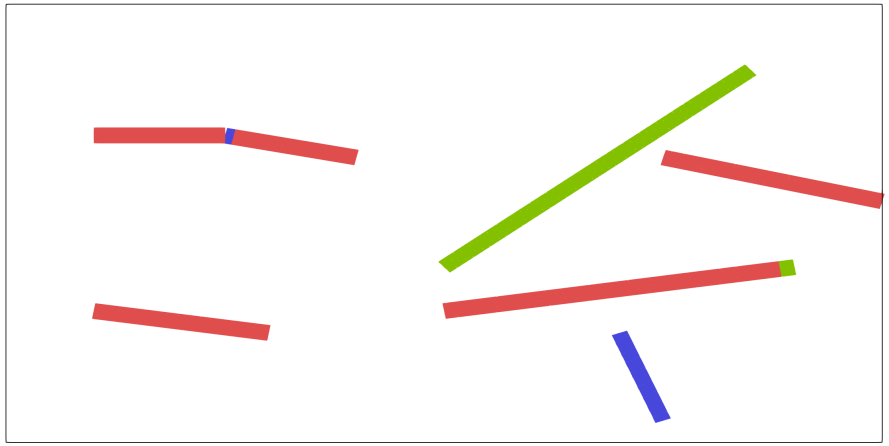

End of Stage 2 at $t = T$

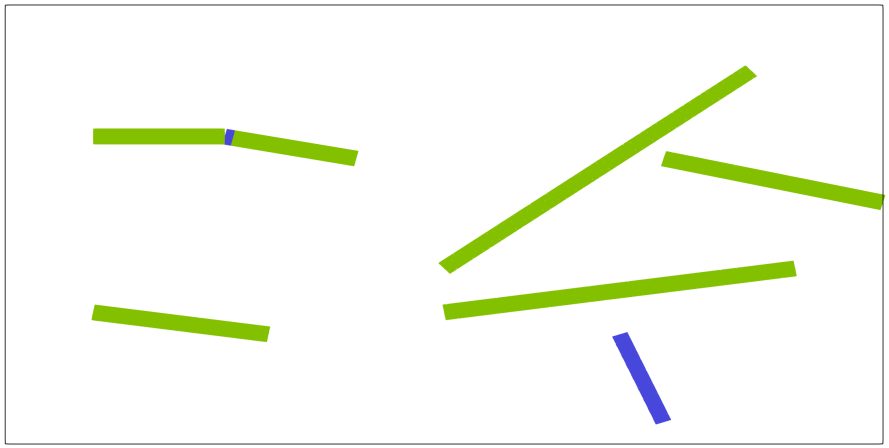

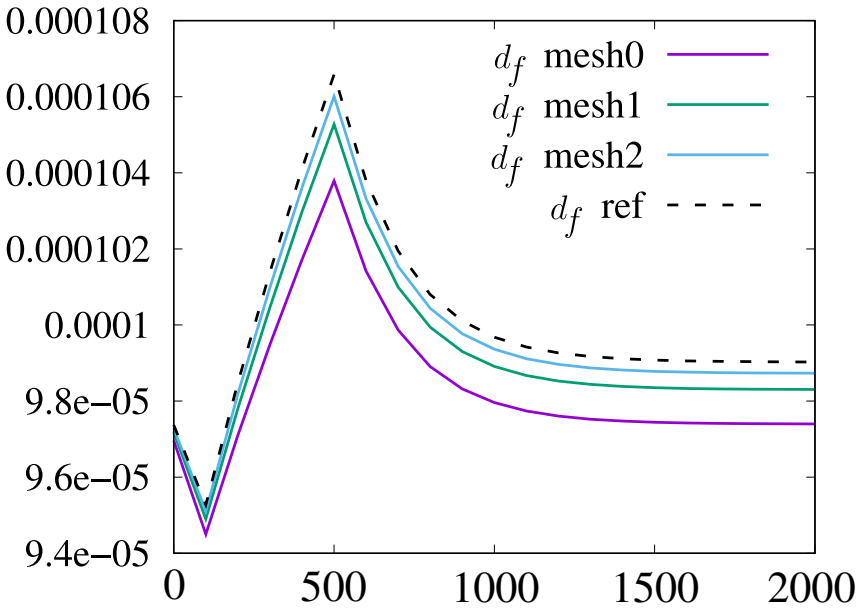

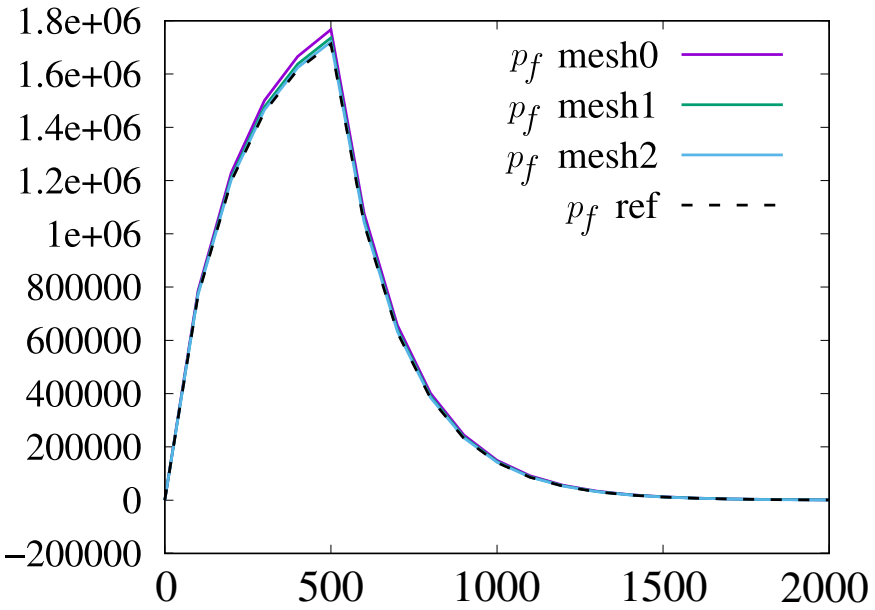

Figure: Mean aperture and mean pressure in fractures as a function of time.

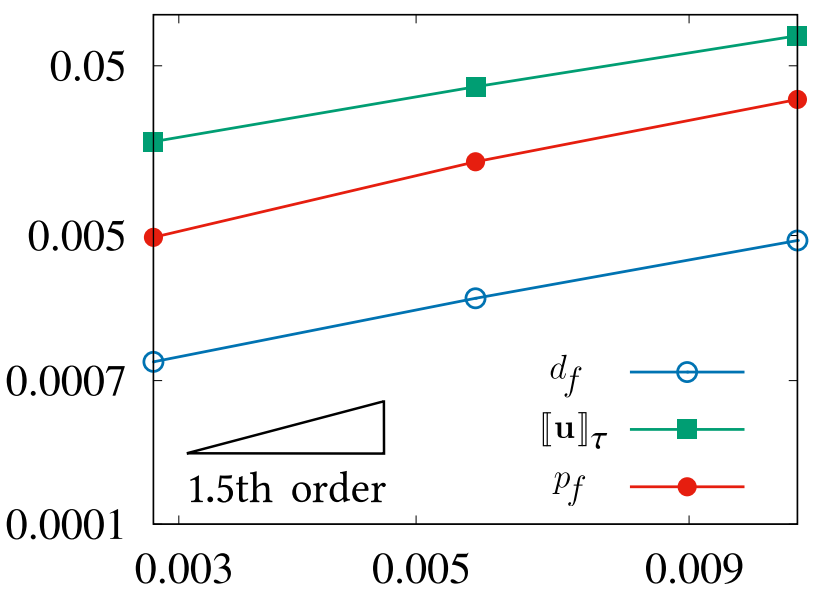

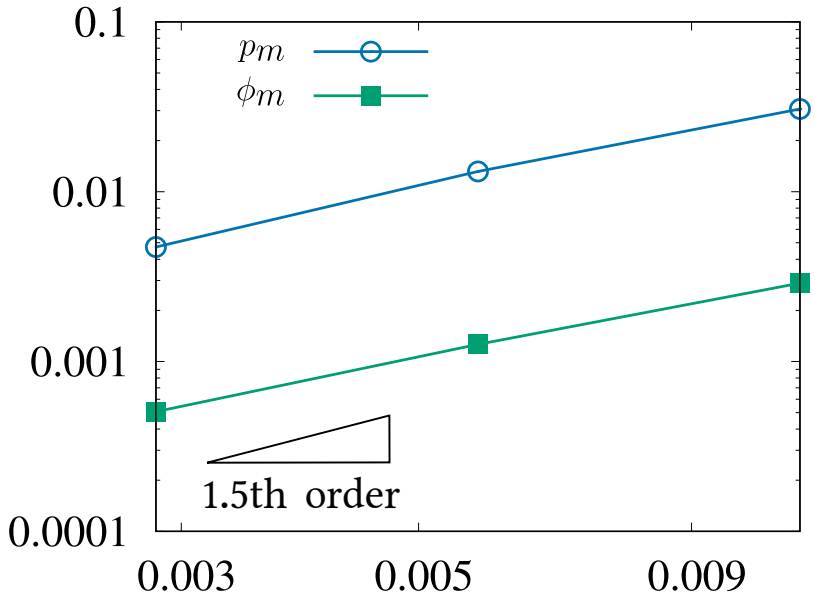

Figure: Relative L_2 error between the current and reference solution

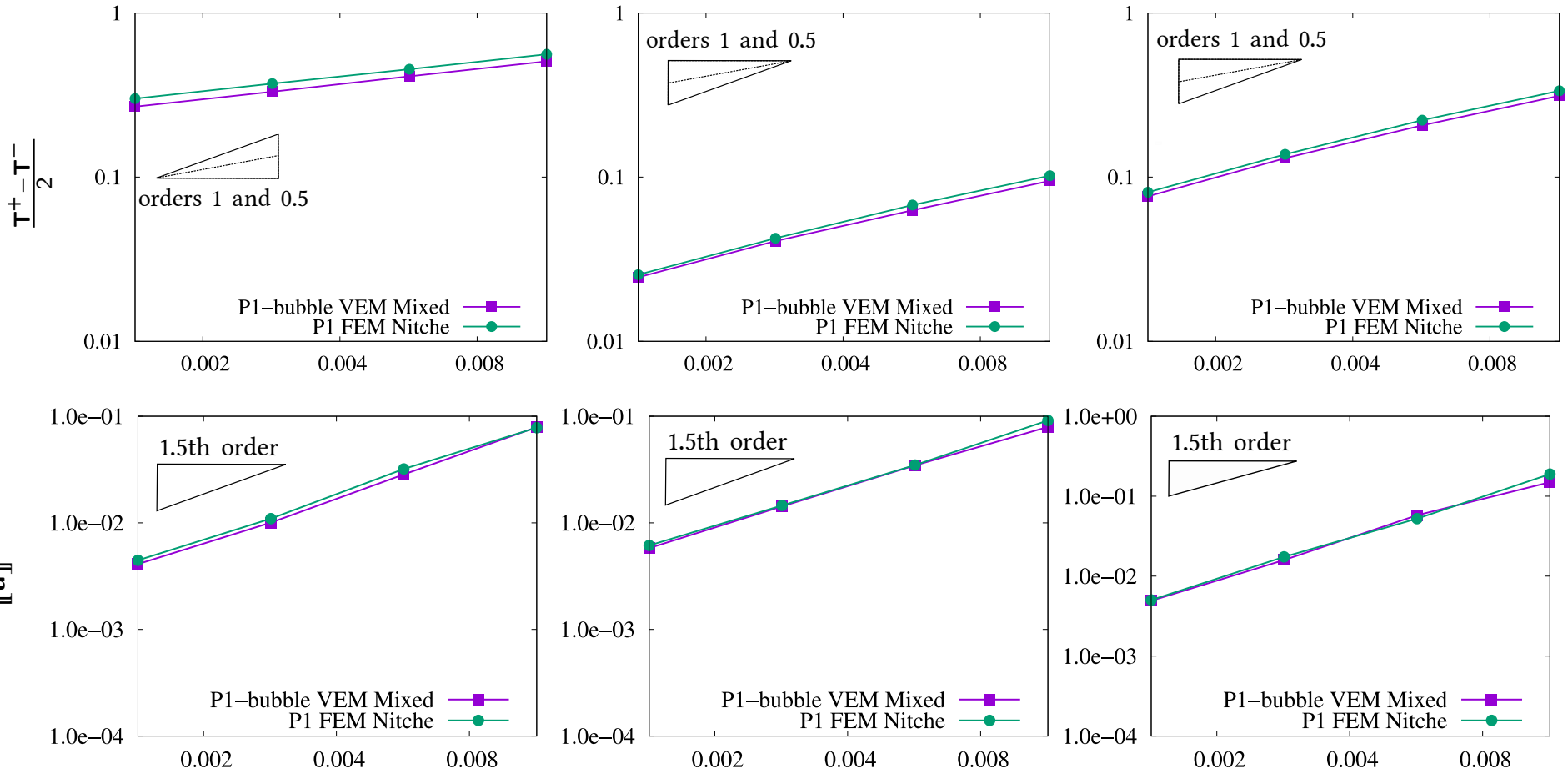

Figure: Relative L_2 error, as a function of the size of the largest fracture face, between the current and reference solutions in terms of $(\mathbf{T}^+ - \mathbf{T}^-)/2$ (top) and $[\![\mathbf{u}]\!]$ (bottom) along fractures 1,2 and 3 from left to right: Mixed $\mathbb{P}^1$-bubble VEM - $\mathbb{P}^0$ vs Nitsche $\mathbb{P}^1$ FEM.

3D DFM poromechanical test case

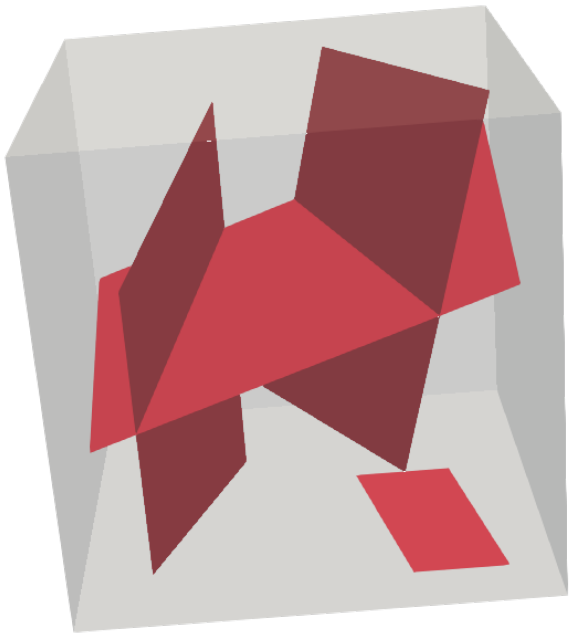

Isotropic permeability tensor:

$$\mathbb{K}_m = 10^{-14}\ \mathbb{I}\,(\mathrm{m}^2)$$

Fracture aperture in contact state:

$$d_f^c(\mathbf{x}) = 10^{-3}\,\mathrm{m}$$

$F = 0.5,\ b = 0.5,\ E = 10$ GPa, $\nu = 0.2$

Initial conditions

Initial pressures $p_m^0 = p_f^0 = 10^5$ Pa

Boundary conditions

Mechanics

Top boundary:

$$\mathrm{u}(t,\mathrm{x}) = \begin{cases} t\,[0.005\,\mathrm{m}, 0.002\,\mathrm{m}, -0.002\,\mathrm{m}]\ 2t/T & \text{if } t \le T/2 \\ t\,[0.005\,\mathrm{m}, 0.002\,\mathrm{m}, -0.002\,\mathrm{m}] & \text{otherwise} \end{cases}$$

Bottom boundary: $\mathbf{u}(t,\mathbf{x}) \equiv \mathbf{0}$
Lateral boundaries: $\sigma^T(t,\mathbf{x})\mathbf{n}(\mathbf{x}) \equiv \mathbf{0}$

Flow

Boundary $y = 0$ and $y = 1$: $p_m(t,\mathbf{x}) \equiv p_m^0 = 10^5$ Pa

All other boundaries: impervious

3D DFM poromechanical test case: contact state

$t = T/2$

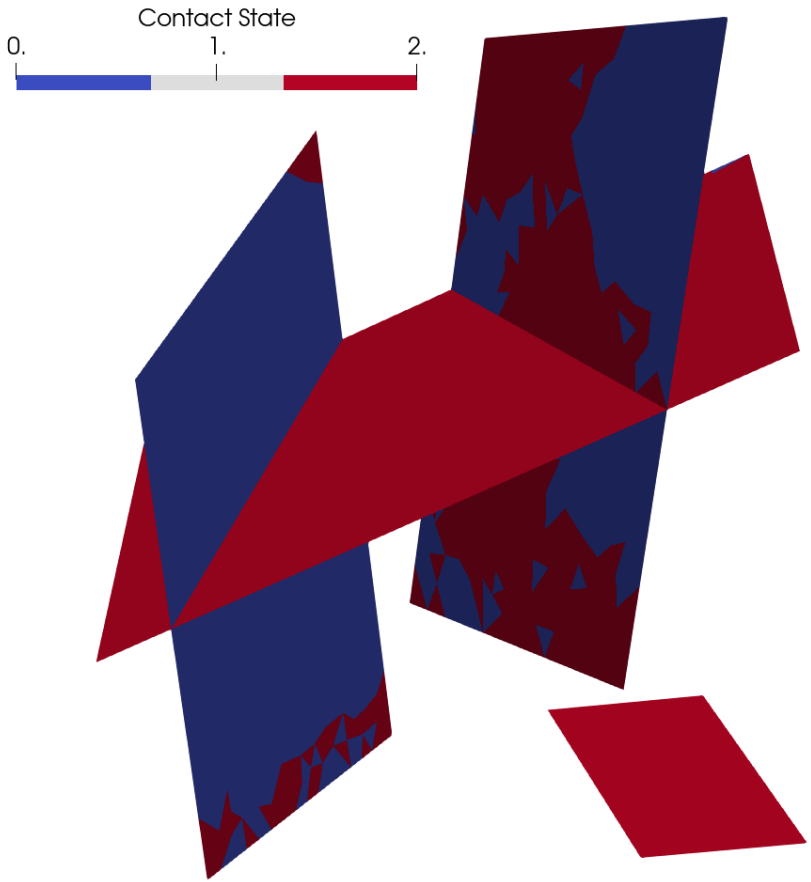

$t = T$

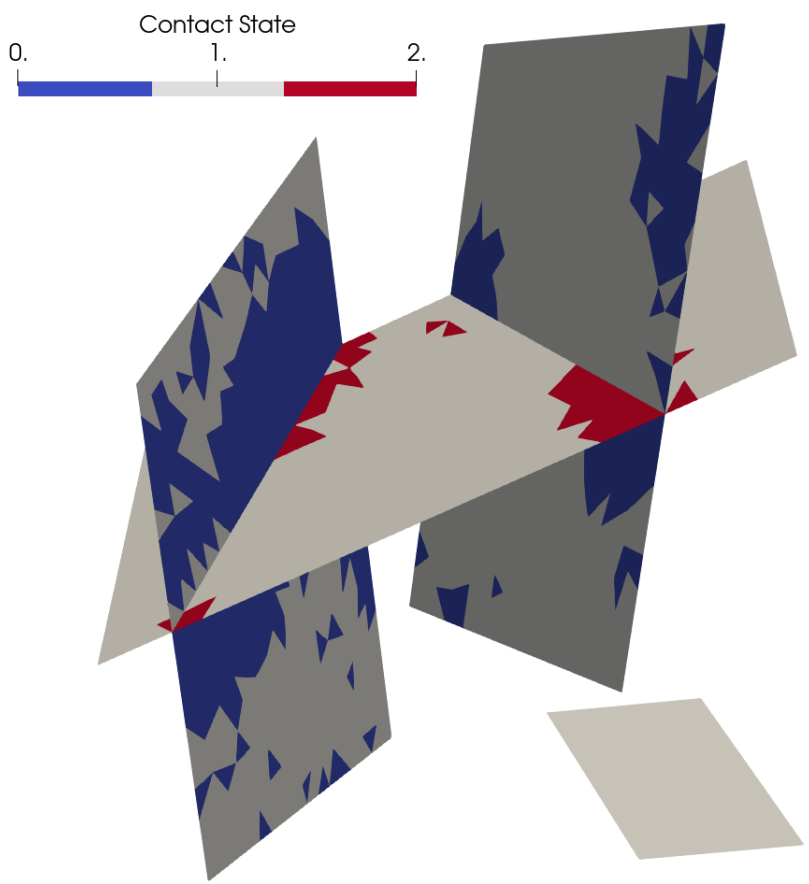

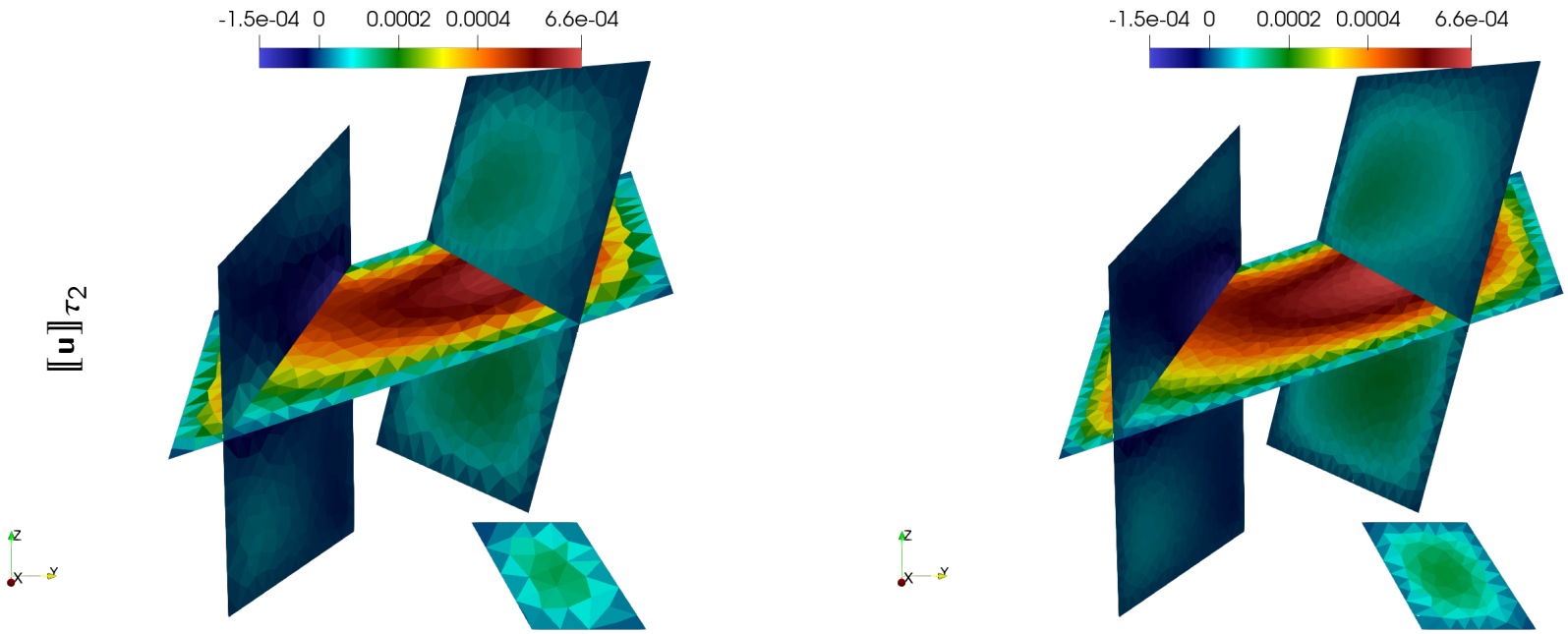

Figure: The τ_2 component of the tangential jump with the 47k cells mesh (left) and the 127k cells mesh (right), obtained at final time.

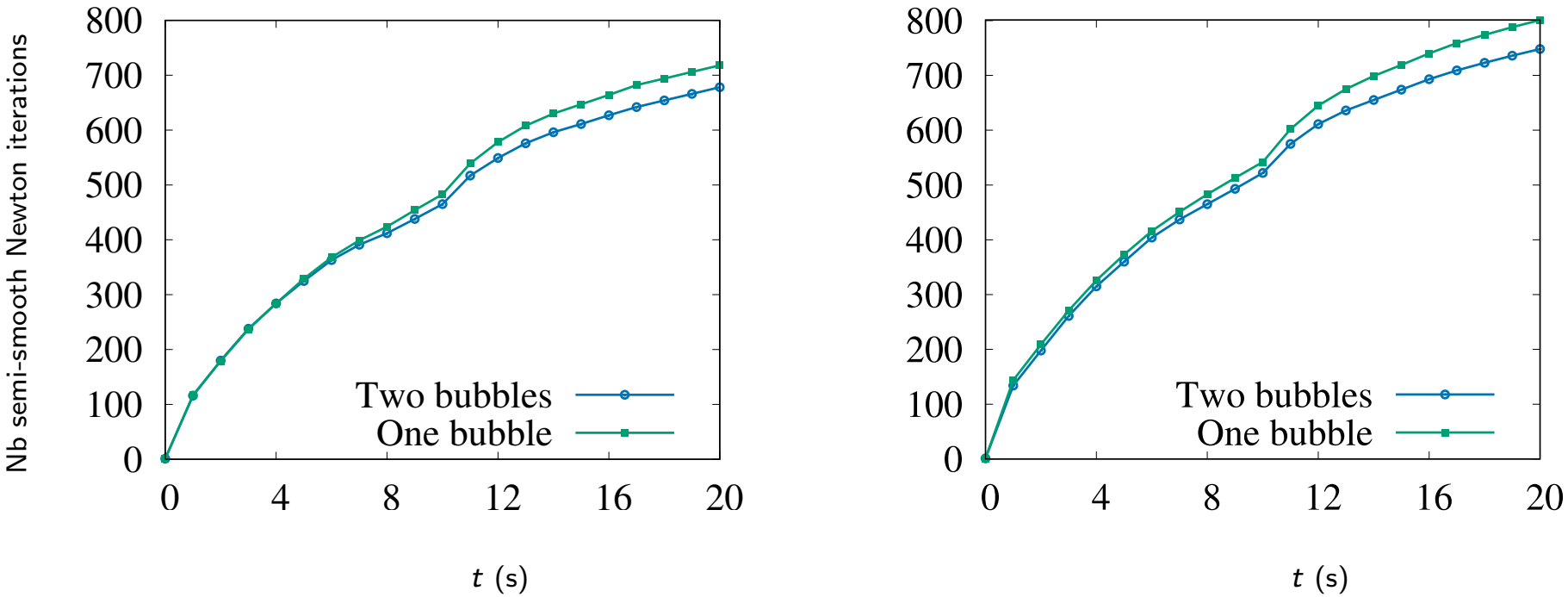

Figure: Total number of semi-smooth Newton iterations for the contact-mechanical model as a function of time, with both one-sided and two-sided bubbles and for both meshes with 47k cells (left) and 127k cells (right).

Conclusions and perspectives

- Extension to polyhedral meshes of the mixed $\mathbb{P}^1$-bubble - $\mathbb{P}^0$ formulation for contact mechanics
- Numerical validation in terms of convergence and robustness on academic test cases

Perspectives:

- More challenging test cases on CPG meshes for CO2 injection in a faulted reservoir
- Higher order polytopal method
- Nitsche's formulation
- Extension to non-matching meshes

Thank you for your attention.